

## Evaluation of The Cathodic Protection Applied to Steel Embedded in the AAS Using the Finite Element Method

W. Aperador<sup>1,\*</sup>, A. Delgado<sup>1,2</sup>, J. Carrillo<sup>1</sup>

<sup>1</sup>Department of Engineering, Universidad Militar Nueva Granada, Carrera 11 No. 101-80, Fax:+57(1) 6343200, Bogotá, Colombia.

<sup>2</sup>Escuela Colombiana de Ingeniería – Julio Garavito, Bogotá, Colombia.

\*E-mail: [g.ing.materiales@gmail.com](mailto:g.ing.materiales@gmail.com)

*Received:* 20 April 2013 / *Accepted:* 10 May 2013 / *Published:* 1 June 2013

---

In the present work using mortar samples of slag activated with alkaline solution (AAS) to which chloride induces a corrosive process by entering the chloride ion. After that cathode protection was applied to steel bars and then applied cathodic protection on steel bars ASTM A706 seismic resistant earthquake resistant embedded in the mortar with and without process of carbonization. For comparative purposes, ordinary Portland cement mortars were used (OPC) and exposed to the same experimental conditions. By means of the design through the numeric method based on finite elements (FEM) and the method of finite difference (FDM) applied to the cathodic protection and the electrochemical system, consists consisting of a simple geometry using the finite difference method (FDM), the influence of the conductivity was investigated on the cathodic protection in the of AAS mortars AAS. The study shows as a result was investigated, obtaining that the carbonation process has a positive influence in the conductivity favoring the cathodic protection.

---

**Keywords:** cathode protection, chloride ion, AAS, finite element method.

### 1. INTRODUCTION

Frequently has been promoted the reinforced concrete structures as a construction with an unlimited life service and with minimum requirements of maintenance. However, in certain unfavorable circumstances this is not certain, as there are some factors that favor the corrosive process causing the despassivation of the steel embedded in the concrete. High corrosion velocities are originated; those can be set serious damage in a short time [1]. This is the case of the bridge decks contaminated with deicing salts [2], of the offshore platforms [3], or the structures exposed to warm climate in marine environment. In aggressive environmental conditions the wear leads to taking

preventive actions by expensive repairs or inclusive or even reach radical decisions as the demolition of the structures that have been affected.

The cathodic protection (CP) is considerate as the only one rehabilitation technique that has demonstrated avoid the corrosion process in the contaminated bridge decks with the salinity of the environment [4-6]. The CP is very useful due that extends the service life of the steel pipes; in special the buried that are used in the transport of oil and gas as well as in structures offshore oil drilling, hoofs seagoing vessels, marine pilings, water tanks and chemical recipients. The concept behind the CP consists in displace the potential of a metal electrode to a value more negative where the corrosion velocity is low enough inhibiting to the corrosive process [7].

In the case of structures base on concrete, is affected by the exposition to aggressive saline environments, the convectional procedure of reparation implies the elimination of the concrete armors contaminated with chlorides; cleaning in the whole perimeter, replacement of the affected concrete and the application of some kind of protection which avoid new repairs [8]. This process is very expensive from the economic standpoint and harmful for both workers and the environment.

There is a very special type of Alkali-activated slag concrete (AAS). This type of concrete is conformed by a mixture of ground granulated slag, fine aggregates, thick aggregates and alkali solution (sodium silicate) in the required quantity for the mixture. Those have been studied object by a large number of researchers in the field of new construction materials [9]. The AAS present technologic and economic advantages in comparison with the traditional Portland cements (OPC), among which stand: lower hydration heat, low permeability, greater high temperature resistance, greater resistance to chemical attack and improvement of the mechanical resistance. Likewise, present some disadvantages such as: faster curing, more formation of microfissures and resistance variability [10]. The reinforced concrete is one of the materials for construction more versatile, for its service properties and wide variety of applications, and low cost. Nevertheless, the rebar in this type of structures has susceptibility to corrode decreasing considerably the service life of the composed material concrete-steel [11-15].

The corrosion in the rebar is one of the causes more likeable of the wear of the concrete structures. In the Portland concretes the free chloride ions trigger corrosion process by pitting; that attack directly the passive layer of the steel and impedes its regeneration.

The aim of this work is applies the cathodic protection (CP) in each system conformed by Alkali-activated slag concrete and exposed to the solution with chlorine ions and determinate its behavior against aggressive environment. Furthermore, a mathematical model was applied based on the finite element method to study the behavior of the CP embedded in AAS and OPC mortars.

## 2. EXPERIMENTAL PROCEDURE

Fort the development of the present study was used: a Colombian steelmaker slag of blast furnace with a chemical composition of 33.7% SiO<sub>2</sub>, 12.8% Al<sub>2</sub>O<sub>3</sub>, 45,4% CaO, 0,5% TiO<sub>2</sub> and 1.00% MgO as cementitious; The basicity coefficient  $(CaO+MgO/SiO_2+Al_2O_3)$  and the quality  $(CaO+MgO+Al_2O_3/SiO_2+TiO_2)$  are 1.0 and 1.73 respectively. As alkali activator a sodium silicate

solution with concentration of 5%  $\text{Na}_2\text{O}$  expressed as percentage by weight of slag. The used aggregates correspond to river sand with density of  $2410 \text{ kg/m}^3$  and 2.9% of absorption. The OPC mixtures used commercial Portland cement without additive. The conformation of the mortar mixtures in both cases content  $400 \text{ kg/m}^3$  of cementitious material dosage. It was assumed that the relation water/cement and solution water+ activating/slag are equivalent, in both cases the relation was 0.4 [16-18].

It was managed mortars mixtures with Alkali Activated Slag without the carbonation process (AAS) and Alkali Activated Slag completely carbonated (AASC). For the process of carbon dioxide inclusion was used in a carbonation chamber at controlled conditions (3%  $\text{CO}_2$ , 65% relative humidity and  $20^\circ\text{C}$  of temperature); for the OPC mortars the conditions were similar to AAS: mortar of ordinary Portland cement without carbonation (OPC) and mortar of ordinary Portland cement carbonated (OPCC). The working conditions for each mixture were:

- Mortar subjected to accelerated carbonation and chloride ion attack. The concretes were immersing in a solution with 3.5% of analytical sodium chloride Panreac PA131655.1211 NaCl 99.0%) for 60 days, subsequently was applied a cathodic protection. The purpose is to begin the process of corrosion with the carbonation; then with the chlorine is performed the propagation process and with the cathodic protection is generated the anticorrosive defense.
- Mortar without accelerated carbonation, with chloride ion exposition and application of cathodic protection.

For the tests were made cylindrical specimens with 12.5 mm of diameter by 25 mm height, with a ASTM A 706 structural steel bar placed in the center of the specimen. The rebar diameter is 6.15 mm. The used electrochemical cell is composed by an auxiliary electrode of stainless steel, a reference electrode of  $\text{Cu}/\text{CuSO}_4$  and as a working electrode the ASTM A 706 structural steel with an exposed area of  $10 \text{ cm}^2$  [19]. The mounting for the cathodic protection implementation is shown in the figure 1. The impressed current applied on the auxiliary electrode (Anode AISI 304 SS) in each one of the cases was  $55 \times 10^{-6} \text{ A cm}^{-2}$ .

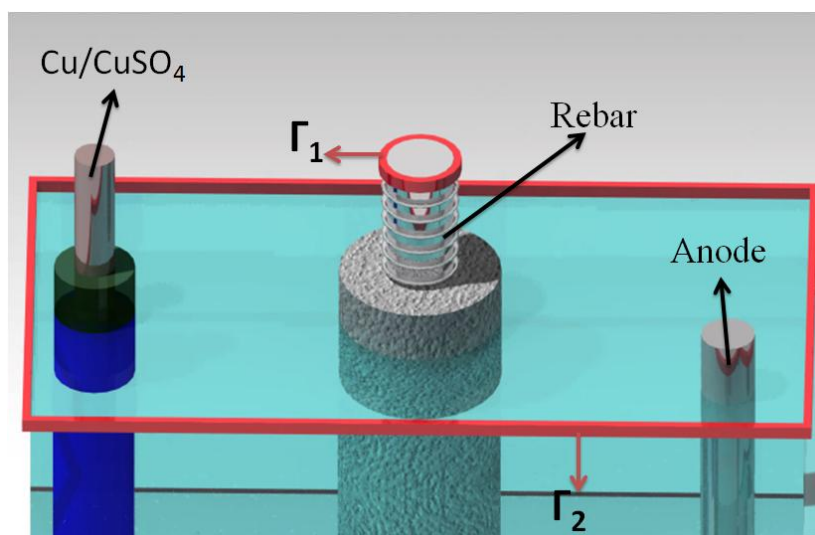


**Figure 1.** Design used in the cathodic protection process.

### 3. RESULTS AND DISCUSSION

#### 3.1 Numeric method

One of the applications of the numeric methods is to predict the behavior of the steel corrosion with a configuration of coplanar electrodes without variations of polarization effects. Analyses were limited to a one-dimensional approach in the rectangular coordinate systems. These mathematical treatments used the Poisson and Laplace equations:

$$\nabla^2\phi = \frac{\partial^2\phi}{\partial x^2} + \frac{\partial^2\phi}{\partial y^2} + \frac{\partial^2\phi}{\partial z^2} = f(x, y, z) \tag{1}$$

Where  $\nabla^2\phi = \frac{\partial^2\phi}{\partial x^2} + \frac{\partial^2\phi}{\partial y^2} + \frac{\partial^2\phi}{\partial z^2} = f(x, y, z)$  correspond to the Laplace and  $f(x, y, z) \neq 0$  for the Poisson equation. The variational formulation for the unidimensional limit is the problem approached by the simplifying of Butler-Volmer equation [20]. Considering the physic situation that is shown in the figure 1, in where a plastic container contents the reinforced mortar and an anode situated at the corner  $x \sim 12.5$  cm and in the y axis  $y \sim 12.5$  cm, the boundary value of this situation is given by the equation 2:

$$-k\Delta\phi = f(x, y) \tag{2}$$

With the boundary condition:  $-k \frac{\partial\phi}{\partial n} = 0$  en  $\Gamma_1$ ,  $y - k \frac{\partial\phi}{\partial n} = h(\phi)$  in  $\Gamma_2$ , where  $h(\phi)$  Is the function that represents the polarization curve of the embedded and immersed rebar in an electrolyte of 3.5% NaCl and  $f(x, y)$  is the impressed current applied to the steel embedded in the mortar (anode) system.

Although  $v$  is part of  $H^1(\Omega)$ ,  $H^m(\Omega) = \{v : \partial_\alpha v \in L^2 \forall \alpha \ni |\alpha| \leq m\}$  and  $L^2(\Omega) = \{f : (\Omega) \rightarrow \Re \mid \int_\Omega |f(x)|^2 < \infty\}$ . If each member of the equation 2 is multiplied by the  $v$  parameter

and is integrated in the  $\Omega$  domain, it is obtained the equation 3:

$$\int kv\Delta\phi = -\int fv \tag{3}$$

Furthermore, if it is applied the Gree's theorem, the equation 3 becomes in the equation 4:

$$\int_\Omega \text{div}(v\nabla\phi)dx - \int_\Omega \nabla\phi \cdot \nabla v dx = -\frac{1}{k} \int_\Omega fv \tag{4}$$

Using the divergence theorem in the equation 4, it is obtained:  $\int_{\Gamma(1)+\Gamma(2)} v\nabla\phi \cdot n - \int_\Omega \nabla\phi \cdot \nabla v dx = -\frac{1}{k} \int_\Omega fv$

$$\tag{5}$$

Applying the boundary conditions, it is found that:

$$\int_{\Gamma(1)+\Gamma(2)} vhd\Gamma - \int_\Omega \nabla\phi \cdot \nabla v dx = -\frac{1}{k} \int_\Omega fv dx, \forall v \in H^1(\Omega) \tag{6}$$

Moreover, if:

$$a(\phi, v) \equiv \int_\Omega \nabla\phi \cdot \nabla v dx \tag{7}$$

and

$$l(v) \equiv \int_{\Gamma(1)+\Gamma(2)} vhd\Gamma + \int_\Omega fv dx \tag{8}$$

Are defining with the classic formulation, which means:

$$a(\phi, v) = l(v), \forall v \in H^1(\Omega) \tag{9}$$

Finding the exact solution in two dimensions is arduous work, therefore is constructed an approximation called  $\phi_N$ , which stands a unidimensional problem in the finite space. One part of the  $\Omega$  domain is divided in  $N$  parts and one finite dimension of sub-space  $H^1(\Omega)$  called  $C_N$  and formed by the function  $\varphi_i : \Omega \rightarrow \mathfrak{R}$ . Where  $\varphi_i$  is a polynomial in  $\mathfrak{R}^2$  (Euclidean vector space bidimensional) for  $i = 1, \dots, N$ .

The problem focuses on finding  $\phi_N \in C_N$ , thus:

$$a(\phi_N, v) = \frac{1}{k}(f, v), \quad \forall v \in C_N \tag{10}$$

As,  $\Phi_i, i=1, \dots, N$  is the base of  $C_N^2$ . Therefore, the solution is expressed as lineal combination of  $\Phi_i$ . Reminding that one of the fundamental tasks of FEM is created and selected an adequate base, hence, if:

$$\phi_N = \sum_{i=1}^{N \times M} a_i \Phi_i \tag{11}$$

It is defined the coefficient  $a_i$  as the unknown quantity to evaluate, in this manner the numeric solutions is simplified to the following expression:

$$\sum_{i=1}^N a_i \int_{\Omega} \left[ \frac{\partial \Phi_i}{\partial x}(x, y), \frac{\partial \Phi_i}{\partial y}(x, y) \right] \cdot [\nabla v(x, y) dA] = \int_{\Gamma(1)+\Gamma(2)} v h d\Gamma + \int_{\Omega} \frac{f(x, y)v(x, y)}{k} dA \tag{12}$$

In particular, although  $v$  is replaced by the base elements, then:

$$\sum_{i=1}^N a_i \int_{\Omega} \left[ \frac{\partial \Phi_i}{\partial x}(x, y), \frac{\partial \Phi_i}{\partial y}(x, y) \right] \cdot \left[ \frac{\partial \Phi_j}{\partial x}(x, y), \frac{\partial \Phi_j}{\partial y}(x, y) dA \right] = \int_{\Gamma(1)+\Gamma(2)} v h d\Gamma + \int_{\Omega} \frac{f(x, y)\Phi_j(x, y)}{k} dA$$

$$j = 1, \dots, N \tag{13}$$

or in matrix form

$$\begin{bmatrix} \int_{\Omega} \frac{\partial \Phi_1}{\partial x} \frac{\partial \Phi_1}{\partial x} + \frac{\partial \Phi_1}{\partial y} \frac{\partial \Phi_1}{\partial y} dx & \dots & \int_{\Omega} \frac{\partial \Phi_N}{\partial x} \frac{\partial \Phi_1}{\partial x} + \frac{\partial \Phi_N}{\partial y} \frac{\partial \Phi_1}{\partial y} dx \\ \vdots & \ddots & \vdots \\ \int_{\Omega} \frac{\partial \Phi_1}{\partial x} \frac{\partial \Phi_N}{\partial x} + \frac{\partial \Phi_1}{\partial y} \frac{\partial \Phi_N}{\partial y} dx & \dots & \int_{\Omega} \frac{\partial \Phi_N}{\partial x} \frac{\partial \Phi_N}{\partial x} + \frac{\partial \Phi_N}{\partial y} \frac{\partial \Phi_N}{\partial y} dx \end{bmatrix} \begin{bmatrix} a_1 \\ \vdots \\ a_N \end{bmatrix} = \begin{bmatrix} \int_{\Omega} f(x, y)\Phi_1 + \int_{\Gamma(1)+\Gamma(2)} \Phi_1 h \\ \vdots \\ \int_{\Omega} f(x, y)\Phi_N + \int_{\Gamma(1)+\Gamma(2)} \Phi_N h \end{bmatrix}$$

$$\frac{1}{k}$$

### 3.2 Distributions of Isopotential Lines

The potential measurements were performed to the reinforced mortar specimens embedded in a 3.3% NaCl electrolyte after 49 day of immersion. In the table 1 are consolidated the used parameters in the numeric simulation. The protection cathodic standards are established by the NACE (-0.85 V vs.

Cu/CuSO<sub>4</sub>) [21]. The potential measurements were registered when the equilibrium conditions were achieved.

**Table 1.** Used design parameters, in the protection of impressed current for the embedded steel bars in mortar AAS and OPC subjected to natural carbonation and accelerated carbonation.

Parameter	Description
<b>AASC Mortar</b>	
Average conductivity of the AASC mortar	0.019 mS cm <sup>-1</sup>
Average conductivity of the electrolyte – 3,5% NaCl	86.3 mS cm <sup>-1</sup>
Localization of the anodes (x,y)	x~12.5 cm; y~12.5 cm
Applied current density on the anodes	55×10 <sup>-6</sup> A cm <sup>-2</sup>
Potential measured after 49 days	-0.892 V vs. Cu/CuSO <sub>4</sub> (CSE)
Anode potential output	0.915 V
<b>OPC Mortar</b>	
Average conductivity of the OPC mortar	0.042 mS cm <sup>-1</sup>
Average conductivity of the electrolyte – 3,5% NaCl	86.3 mS cm <sup>-1</sup>
Localization of the anodes (x,y)	x~12.5 cm; y~12.5 cm
Applied current density on the anodes	55×10 <sup>-6</sup> A cm <sup>-2</sup>
Potential measured after 49 days	-0.943 V vs. Cu/CuSO <sub>4</sub> (CSE)
Anode potential output	0.915 V
<b>AAS Mortar</b>	
Average conductivity of the AAS mortar	0.086 mS cm <sup>-1</sup>
Average conductivity of the electrolyte – 3,5% NaCl	86.3 mS cm <sup>-1</sup>
Localization of the anodes (x,y)	x~12.5 cm; y~12.5 cm
Applied current density on the anodes	55×10 <sup>-6</sup> A cm <sup>-2</sup>
Potential measured after 49 days	-0.952 V vs. Cu/CuSO <sub>4</sub> (CSE)
Anode potential output	0.915 V
<b>OPCC Mortar</b>	
Average conductivity of the OPCC mortar	0.23 mS cm <sup>-1</sup>
Average conductivity of the electrolyte – 3,5% NaCl	86.3 mS cm <sup>-1</sup>
Localization of the anodes (x,y)	x~12.5 cm; y~12.5 cm
Applied current density on the anodes	55×10 <sup>-6</sup> A cm <sup>-2</sup>
Potential measured after 49 days	-0.897 V vs. Cu/CuSO <sub>4</sub> (CSE)
Anode potential output	0.915 V

In the figure 1 is shown the experimental scheme using for numeric simulation. A impressed current of 55×10<sup>-6</sup> A cm<sup>-2</sup> is applied, using as anode a stainless steel (AISI 304) electrode with a diameter of 9 mm. The Ω domain is divided in 925 constant elements. The Gauss-Seidel method

resolves the established system. The approximation mathematical function used in each one of the embedded steels in the mortars is:

$$f(x, y) = -r \exp \left[ -s^* (x - x_0)^2 - s^* (y - y_0)^2 \right] \tag{15}$$

Where  $r$  is a factor that involves the polarization potential of the steel bar,  $s^*$  is the factor which relates the anode diameter,  $x_0$  and  $y_0$  are the rectangular coordinates of the ASTM 706 steel bar center.

In the figure 2 and 3 are observed the iso-potential lines distribution of the embedded rebar in an AASC mortar with a potential variation among the lines of 0.2 vs reference electrode. The bar is protected according to the criteria of potential value indicating between -0.85 and -1.0 V vs. reference electrode. In the case of AASC, the figure 2 and 3, the impressed current of  $55 \times 10^{-6} \text{ A cm}^{-2}$  generates a potential change of 4 volts vs. reference electrode approximately indicating that the structure is protected against the corrosion. However, it is possible to observe that by applying a less impressed current quantity for the embedded steel in AASC is generated a good cathodic protection as well [22].

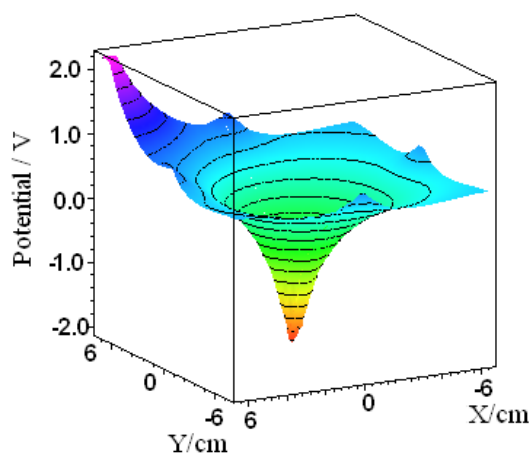


**Figure 2.** Calculation of potential distribution for AASC mortars, for a bidimensional model.

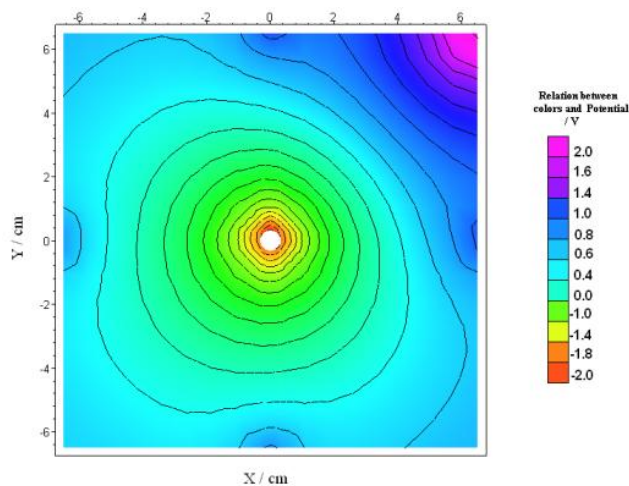


**Figure 3.** Calculation of iso-potential lines distribution applying rectangular coordinates for the steel bar embedded in AASC mortar.

In the figure 4 and 5 is observed the calculation and the distribution of iso-potential lines of the embedded rebar in an AAS mortar, it is obtained a potential difference of 0.2 V vs. reference electrode. The cathodic protection reached in the AAS is 1 V vs. reference electrode. This result leads to stand that the impressed current protects the structure cathodically [23].

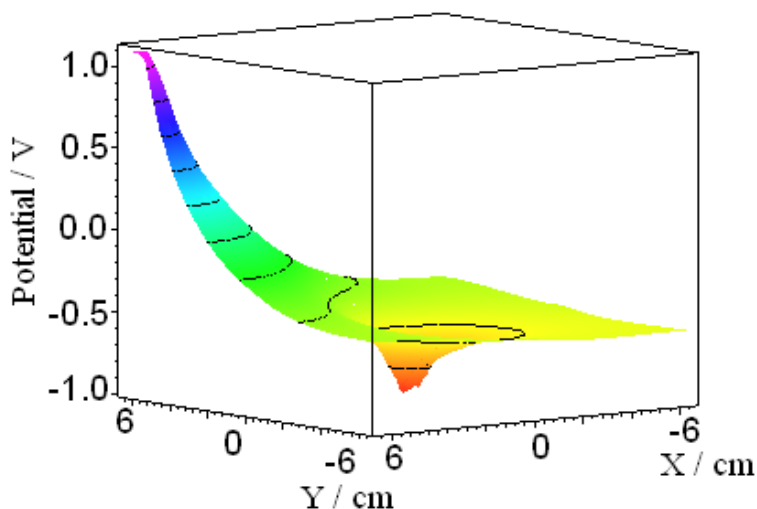


**Figure 4.** Calculation of potential distribution for AAS mortars using a bidimensional model.

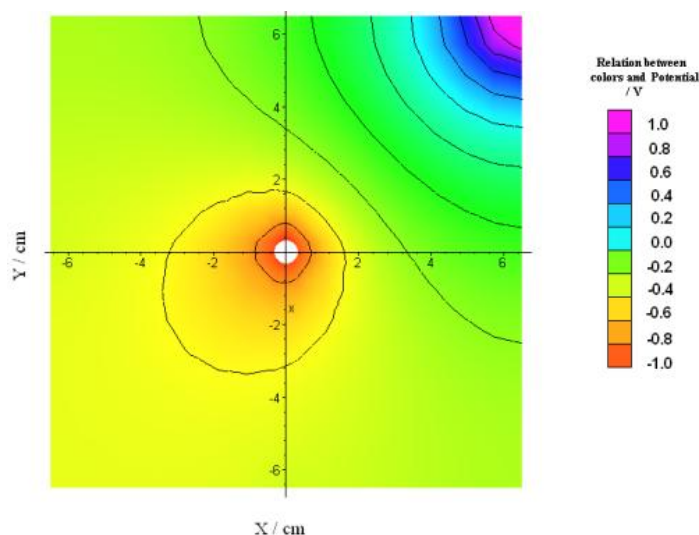


**Figure 5.** Calculation of iso-potential lines distribution by rectangular coordinates for the steel bar embedded in AAS mortar.

In the figure 6 and 7 is observed the calculation and the distribution of the iso-potential lines of the embedded rebar in an OPCC mortar. It is obtained a potential difference of 0.2 V vs. reference electrode as well as for the AASC specimen. The impressed current of  $55 \times 10^{-6} \text{ A cm}^{-2}$  generates a potential change of 1.5 Volts vs. reference electrode approximately, indicating an adequate cathodic protection. It is important to emphasize the use of lower current value [24].

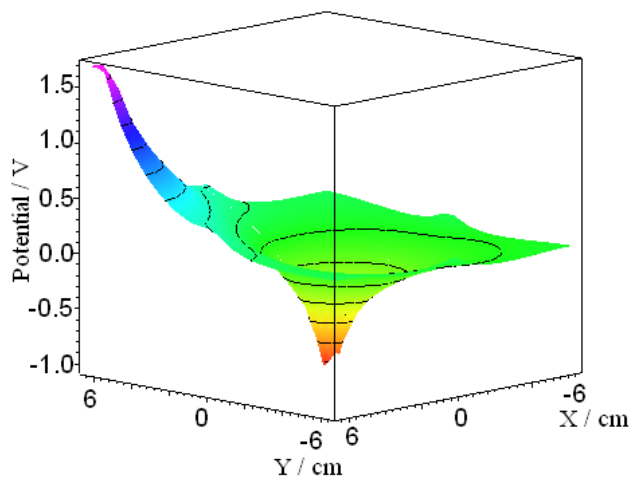


Figure 6. Calculation of potential distribution for OPCC mortars using a bidimensional model.

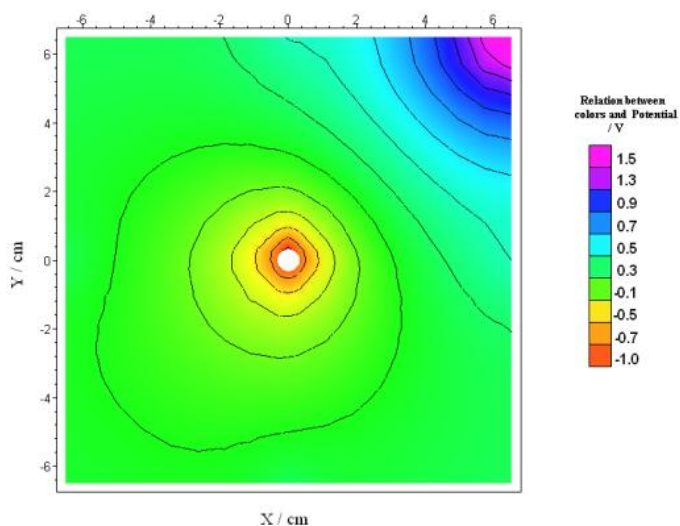


Figure 7. Calculation of iso-potential lines distribution by rectangular coordinates for the steel bar embedded in OPCC mortar.

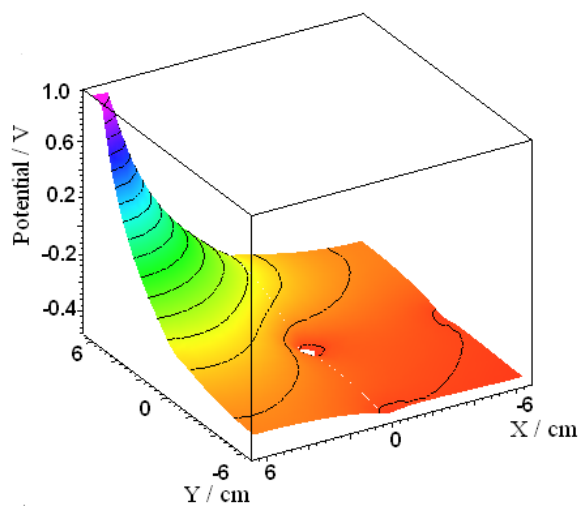
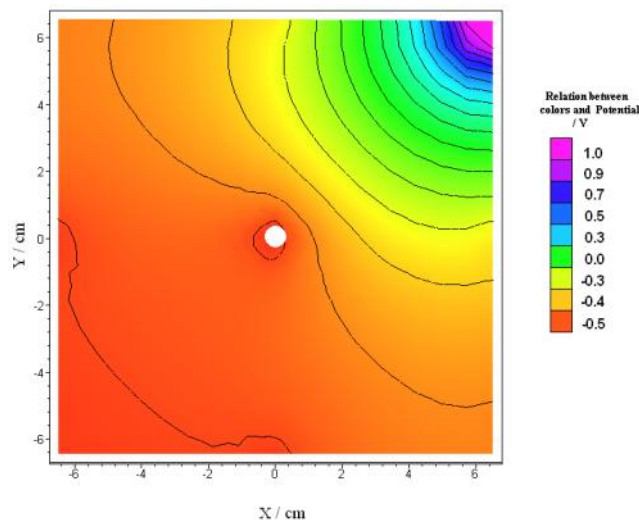


Figure 8. Calculation of potential distribution for OPC mortars using a bidimensional model.



**Figure 9.** Calculation of iso-potential lines distribution by rectangular coordinates for the steel bar embedded in OPC mortar.

In the figure 8 and 9 is observed the calculation and distribution of the iso-potential lines of the embedded rebar in the OPC mortar. It is obtained a potential difference of 0.1 V vs. reference electrode. The cathodic protection indicates a potential of 1 V vs. reference electrode; this shows that with the impressed current the structure is cathodically protected [25].

#### 4. CONCLUSIONS

Este resultado es de gran importancia en el empleo en ingeniería del proceso de protección catódica para disminuir la energía utilizada en estructuras de concreto. Adicionalmente mediante los modelos matemáticos y el cálculo FEM se permite evaluar el rendimiento de la PC usando el parámetro de la conductividad. Por último la técnica de protección catódica permite concluir que el proceso de carbonatación tiene una influencia positiva en la conductividad el cual es el parámetro de diseño que favorece la implementación de esta técnica.

The AASC mortar presents the highest conductivity value (twelve times superior than OPCC) which is the responsible of the good cathodic protection generated in this material. The mortars OPC and AAS have a higher conductivity value (0.042 for the OPC and 0.086 for the AAS) indicating that the necessary current increases to generation of the cathodic protection. This result is of great importance to the engineering of the cathodic protection process, to decrease the used energy in concrete structures. Furthermore, using mathematical model and the FEM calculation, is allowed to evaluate the PC performance by conductivity parameters. Lastly, the cathodic protection technique allows standing that the carbonation process has a positive influence in the conductivity which is the design parameter that favors the implementation of this technique.

#### References

1. J. A González, S. Feliú, P. Rodríguez, E. Ramírez, C. Alonso, C. Andrade, *Materials and Structures*, 29 (1996), 40.

2. J. G Newton, J. M Sykes, *Corrosion Science*; 28 (1989) 1051.
3. R. D Brownea, R. Blundell, *Nuclear Engineering and Design*, 20 (1972), 429.
4. B. S. Wyatt, *Corrosion Science*, 35 (1993) 1601.
5. A. M Hassanein, G. K Glass, N. R Buenfeld, *Cement and Concrete Composites*, 24 (2002) 159.
6. Xu Jing, Yao Wu, *Construction and Building Materials*, 25 (2011) 2655.
7. J.H Morgan, *Journal of Electroanalytical Chemistry and Interfacial Electrochemistry*, 118 (1981) 251.
8. N. Hackerman, *Langmuir* , 3 (1987) 922.
9. S. Caijun, *Cement Concrete Res*, 26 (1996) 1789.
10. S. Caijun, Q. Jueshi, *Conservation and Recycling*, 29 (2000) 195.
11. M. Holloway, J. M Sykes, *Corrosion Science*, 47 (2000) 3097.
12. A. Allahverdi, B. Shaverdi, B. Kani, *International Journal of Civil Engineering*, 8 (2010) 304.
13. W. Aperador, R. Vera, A. M. Carvajal, *Int. J. Electrochem. Sci.*, 7 (2012) 12870.
14. F. Puertas, *Materiales de Construcción*, 45 (1995) 53.
15. E. P. Reyes-Diaz, E. Maldonado, F. Almeray, D. M. Bastidas, M. Baltazar, J. Chacón, A. Martínez-Villafañe, J. M. Bastidas, C. Gaona Tiburcio, *Int. J. Electrochem. Sci*, 6 (2011) 1892.
16. W. Aperador, R. Mejía de Gutiérrez, D. M Bastidas, *Corrosion Science*, 51 (2009), 2027.
17. W. Aperador, E. Delgado, E. Vera, *Revista Ingeniería de Construcción*, 26 (2011) 81.
18. W. A Chaparro, J.H.B Ruiz, R De Jesús Torres Gómez, *Materials Research*, 15 (2012) 57.
19. ASTM A706/A706M - 09b Standard Specification for Low-Alloy Steel Deformed and Plain Bars for Concrete Reinforcement, Vol. 1.04, Filadelfia (EE.UU.): American Society for Testing and Materials, (2009).
20. R. Montoya, W. Aperador, D.M. Bastidas, *Corrosion Science*, Volume 51, Issue 12, December 2009, Pages 2857–2862
21. NACE Standard RP0290-90 (1990) Item No. 53072.
22. W. Aperador; A. Delgado, J. Bautista, *Ingeniería y Universidad*, 16 (2012) 77.
23. G.T.Parthiban, K.Bharanidharan, D.Dhayanand, Thirumalai Parthiban, N.Palaniswamy, V.Sivan, *Int. J. Electrochem. Sci.*, 3 (2008) 1162 – 1168.
24. A.S.S.Sekar, V.Saraswathy, G.T.Parthiban, *Int. J. Electrochem. Sci.*, 2 (2007) 872 – 882.
25. Ha-Won Song, Velu Saraswathy, *Int. J. Electrochem. Sci.*, 2 (2007) 1- 28.